



Adsolubilisation of thiacloprid pesticide into the layered zinc hydroxide salt intercalated with dodecyl sulphate, for controlled release formulation

Zuhailimuna Muda, Norhayati Hashim, Illyas Md Isa, Suzaliza Mustafar, Suriani Abu Bakar, Mazidah Mamat & Mohd Zobir Hussein

To cite this article: Zuhailimuna Muda, Norhayati Hashim, Illyas Md Isa, Suzaliza Mustafar, Suriani Abu Bakar, Mazidah Mamat & Mohd Zobir Hussein (2019): Adsolubilisation of thiacloprid pesticide into the layered zinc hydroxide salt intercalated with dodecyl sulphate, for controlled release formulation, Materials Research Innovations, DOI: [10.1080/14328917.2019.1655620](https://doi.org/10.1080/14328917.2019.1655620)

To link to this article: <https://doi.org/10.1080/14328917.2019.1655620>



Published online: 21 Aug 2019.



Submit your article to this journal [↗](#)



Article views: 32



View related articles [↗](#)



View Crossmark data [↗](#)



Adsolubilisation of thiacloprid pesticide into the layered zinc hydroxide salt intercalated with dodecyl sulphate, for controlled release formulation

Zuhailimuna Muda^a, Norhayati Hashim^{a,b}, Illyas Md Isa^{a,b}, Suzaliza Mustafar^a, Suriani Abu Bakar^{b,c}, Mazidah Mamat^{a,d} and Mohd Zobir Hussein^e

^aDepartment of Chemistry, Faculty of Science and Mathematics, Universiti Pendidikan Sultan Idris, Tanjong Malim, Malaysia; ^bNanotechnology Research Centre, Faculty of Science and Mathematics, Universiti Pendidikan Sultan Idris, Tanjong Malim, Malaysia; ^cDepartment of Physics, Faculty of Science and Mathematics, Universiti Pendidikan Sultan Idris, Tanjong Malim, Malaysia; ^dPusat Pengajian Sains Asas, Universiti Malaysia Terengganu, Kuala Terengganu, Malaysia; ^eMaterials Synthesis and Characterization Laboratory, Institute of Advanced Technology, Universiti Putra Malaysia, Serdang, Malaysia

ABSTRACT

Sodium dodecyl sulphate surfactant was intercalated into the layered zinc hydroxide salt for the successful adsolubilisation of poor water-soluble pesticide, thiacloprid. The intercalation of the dodecyl sulphate ion was confirmed by PXRD analysis with basal spacing 30.1 Å. The presence of thiacloprid into the interlayer gallery of zinc layered hydroxide also supported with Fourier transform infrared spectra and elemental analysis. Based on the thermal study, thiacloprid was thermally stable after the adsolubilisation compared to its solid form. The release of thiacloprid anions from the nanocomposite into an aqueous solution of sodium phosphate was governed by first-order kinetics. Whereas the release of thiacloprid into sodium sulphate and sodium chloride solution governed by parabolic diffusion kinetics model. In consideration of the obvious breakthrough made in the nanocomposite characterisation and release study, this nanocomposite could be a promising candidate for the profitable improvement of an environment-friendly pesticide formulation.

ARTICLE HISTORY

Received 28 May 2019
Accepted 7 August 2019

KEYWORDS

Adsolubilisation; sodium dodecyl sulphate; thiacloprid; controlled release formulation; intercalation; zinc hydroxide salt; characterization; kinetic study

Introduction

Layered material nanocomposite can be prepared by inserting guest molecule into the interlayer of layered host. Recently, layered material like layered hydroxide salt (LHS) and layered double hydroxide (LDH) are often used as a host or carrier for various guest species, for example 3-(4-methoxyphenyl)propionate [1], graphene [2], anticancer drug; raloxifene hydrochloride [3], mefenamic acid [4], amoxicillin trihydrate [5], diclofenac [6], and chlorpyrifos [7].

Both LDH and LHS have anion exchange properties in order to balance the positive charge of the layers [8,9]. The capability of anionic exchange of these layered materials may be merged to intercalate the surfactant anions inside the interlayer gallery in an attempt to create organo-layered materials [9,10]. Several attempts have been made to intercalate surfactant like dodecyl sulphate (DDS) and dodecylbenzenesulfonate ion into the interlayer of LDH and LHS [7,9,11,12]. DDS can act as a hydrophobic region for enhancing the water dispersed of pesticide and in assistance for adsolubilisation into the interlayer gallery of layered material. The presence of alkyl chain of surfactant is being able to expand the layer thickness reflect on its large molecular weight [9,13]. Therefore, it is easier to intercalate poor water-soluble pesticide into the interlayer of LDH or LHS.

Thiacloprid, (Z)-3-(6-chloro-3-pyridylmethyl)-1,3-thiazolidin-2-ylidenecyanamide belongs to a relatively new class of insecticide [7]. Several studies of environmental behaviour of thiacloprid showed that the molecule has

poor water interaction either at acidic, neutral or alkaline medium [14]. It has a relatively low water solubility, which is only 184 mg L⁻¹ and excellent chemical stability in water [15]. Due to this complication, thiacloprid insecticides enter agricultural surface waters, where they may affect predator-prey interactions, which are of central importance for ecosystems as well as the functions these systems provide [16,17]. Therefore, it is sensible to modify the zinc layered hydroxide (ZLH) with intercalated sodium dodecyl sulphate (SDS) anion in order to improve the adsolubilisation of thiacloprid anion. The release of the thiacloprid was done in aqueous medium of phosphate, sulphate and chloride, and their release behaviour was studied. As far as the authors are aware, there is no work carried out on adsolubilisation of thiacloprid pesticide into the layered zinc hydroxide salt intercalated with DDS, for controlled release formulation. This work is expectant to reveal the potential application of ZLH as the host for the insecticide by concentrating on its controlled release behaviour.

Method

Materials

Each chemical utilised in this synthesis was attained from several chemical providers and used without additional purification. All solutions were prepared using deionised water. SDS and zinc nitrate (Zn(NO₃)₂ · 6H₂O) were purchased from System, Malaysia. Sodium hydroxide (NaOH) was purchased from HmbG Chemicals. Whereas thiacloprid pesticide, C₁₀H₉ClN₄S (THI) was purchased from Nanjing Essence Fine-Chemical.

Synthesis of ZLH-SDS-THI

The ZLH-SDS-THI nanocomposite was synthesised in two steps. First, zinc layered hydroxide-sodium dodecyl sulphate (ZLH-SDS) was synthesised beforehand by co-precipitation method goes by a practice published elsewhere [7] with a few modifications. Concisely, ZLH-SDS was synthesised by the slow addition of 1.0 M NaOH and 40 mL of 0.5 M of $\text{Zn}(\text{NO}_3)_2 \cdot 6\text{H}_2\text{O}$, into a solution containing 40 mL of 0.25 M SDS under magnetic stirring. The pH value was adjusted to 6.5. The slurry was then centrifuged and dried in an oven at 70°C.

The second step involves the preparation of thiachloprid (THI) intercalated into the interlayer of ZLH-SDS (indicated as ZLH-SDS-THI) that was achieved by an ion exchange method. Various concentrations of thiachloprid solution were prepared at 0.0005, 0.001 and 0.0025 M. 0.5 g of previously synthesised ZLH-SDS was dissociated in thiachloprid solution and kept under magnetic stirrer for 2 ½ h. The slurry was then aged for 24 h in an oil bath shaker at 70°C. Then, the slurry was centrifuged and the final white solid was dried in an oven for 24 h.

Characterisation

There are several instruments involved in the characterisation of the ZLH-SDS-THI nanocomposites. The X-ray powder diffraction patterns (PXRD) were obtained using a power diffraction Bruker AXS (model D8 Advance, wavelength of 1.5406 Å) with CuKα radiation at 60 kV and a current of 60 mA. The recorded region of 2θ was from 2° to 60° with a scanning rate of 2° min⁻¹. The Fourier transform infrared (FTIR) spectra were collected in a Thermo Nicolet 6700 Fourier Transform Infrared Spectrometer in the range 400–4000 cm⁻¹ with a resolution of 4 cm⁻¹. The thermal analyses measurement (TGA/DTG) of the sample was obtained with Perkin Elmer Pyris 1 TGA Thermo Balance with a heating rate of 20°C min⁻¹ (N₂ flow rate is 50 mL/min, temperatures of 25–900°C at a rate of 10 K/min). An inductive coupled plasma optical emission spectrometry (ICP-OES), model Agilent, 720 Axial and (CHNO-S), model Thermofinnigan, Flash EA 1112 was used to study the composition of the samples. The surface morphology of the sample was observed by a field emission scanning electron microscope Hitachi model SU 8020 UHR. Surface characterisation of the nanocomposites was carried out by the nitrogen gas adsorption-desorption technique at 77 K using a Quantachrome Autosorb-1 and degassed in an evacuated heated chamber at 120°C overnight.

Release study of nanocomposite

Na_3PO_4 , Na_2SO_4 and NaCl solutions were prepared with various concentrations which are 0.10, 0.20 and 0.30 M. The releases of thiachloprid from the layered material nanocomposites were studied by adding a 0.6 mg sample into the cuvette which is the optimum mass for ion exchange capacity as already be done in the previous study [18]. The instrument of UV-vis was set up with correct data for analyses. The quantity of pesticides released into the solution was measured at the preset time with $\lambda_{\text{max}} = 241.5$ nm.

Results and discussion

PXRD analysis

Figure 1 shows the PXRD patterns for ZLH-SDS, pristine thiachloprid anions and the resulting ZLH-SDS-THI nanocomposite. The diffraction peak of ZLH-SDS, at 9.8 Å corresponding to NO_3^- , which was characterised by a major basal reflection caused by the (200) plane of the monoclinic structure [19]. Whereas the peak at 33.0 Å has the same pattern with layered double hydroxide-sodium dodecyl sulphate (LDH-SDS) that previously reported elsewhere [12]. The resulted ZLH-SDS was completely crystallised without impurities, for instance, ZnO. Based on the equation present by Moezzi et al. [20] (Equations (1) and (2)), the zinc species undergo hydrolysis reactions as zinc nitrate hexahydrate dissolved in water. Liang et al. [21], have represented the main reaction that zinc hydroxide species transform into ZnO nanoparticles (3). In the presence of DDS ions, these zinc hydroxide species could cause

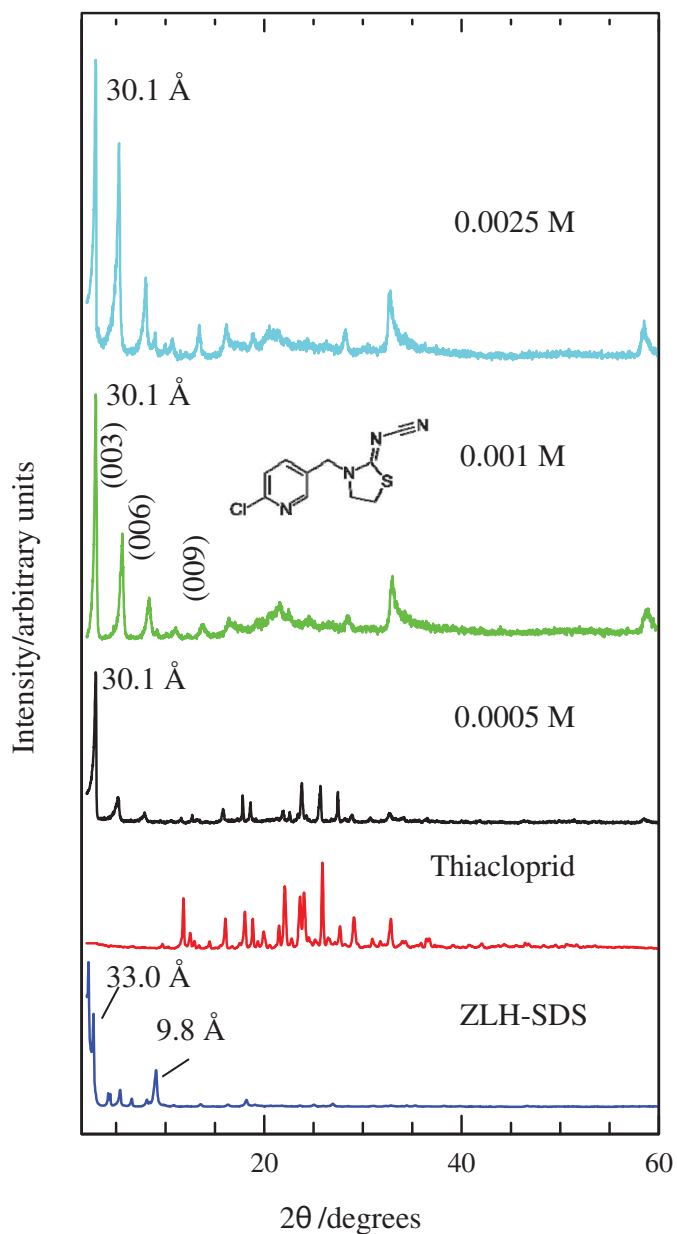
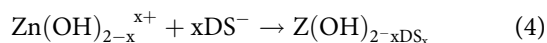
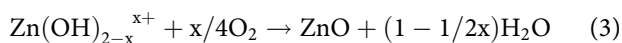
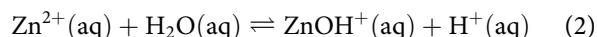
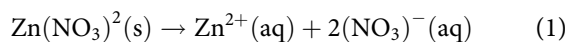


Figure 1. PXRD pattern for ZLH-SDS, thiachloprid anion and ZLH-SDS-THI nanocomposite with concentration of 0.0005, 0.001 and 0.0025 M of thiachloprid.

charge-assemblies to form zinc hydroxide-dodecyl sulphate layered nanosheets (4).



The ZLH-SDS-THI diffraction peak in Figure 1 shows that the nanocomposite presented a well-ordered nanolayered structure with an expanded basal spacing of 30.1 Å for 0.0005, 0.001 and 0.0025 M of thiocloprid anion. After the adsolubilisation of thiocloprid into the interlayer of ZLH, the basal spacing showed a slightly decreased due to the adoption of different orientation angle [22]. The adsolubilisation was apparently proved by the appearance of three harmonic reflections (003, 006 and 009 planes) at the lower 2θ angle which was linked to the basal distance of the nanolayer. The abnormal pattern around 30–40 Å corresponded to the turbostratic effect generated by broadening of basal reflections and the geometry of other diagonal planes, that is in agreement with the prior study as reported elsewhere [23]. As shown in the figure, the intensity of the intercalation peak of ZLH-SDS-THI nanocomposite increased as the concentration of thiocloprid increased from 0.0005 to 0.0025 M which indicated the increasing of crystallinity. This was due to the stronger electrostatic interaction between thiocloprid and ZLH as the concentration of thiocloprid increased which promoted the formation of crystals [23]. As a result of the complete exchange of the nitrate anion, ZLH-SDS-THI nanocomposite prepared using 0.0025 M anion produced sharp, symmetrical and intense peaks. This particular sample was then chosen as the phase pure well-ordered nanocomposite material and used for further characterisations.

FTIR analysis

The FTIR spectra for ZLH-SDS, pure thiocloprid and the ZLH-SDS-THI nanocomposite are shown in Figure 2. All of the bands assigned to thiocloprid, ZLH-SDS, and the ZLH-SDS-THI nanocomposite are outlined in Table 1. As shown in thiocloprid spectra, the peak appeared at 2211, 1098 and 606 cm⁻¹ are due to stretching vibration of C≡N, C-N and C-Cl, respectively. Whereas the peak appeared at 1385 cm⁻¹ is assigned to bending vibration of aliphatic group.

The FTIR spectra of ZLH-SDS shows a strong and sharp absorption band around 3500–3700 cm⁻¹ corresponds to the stretching vibrations of the OH group of the free water molecule [24]. Whereas a strong and broad absorption band centred at 3461 cm⁻¹ attributes to the OH vibration. This band has a broad base due to hydrogen bonds established with the hydration water molecule [8]. Another bending vibration at 1637 cm⁻¹ is the H-O-H bending of water molecule in the interlayer of ZLH-SDS. Two main doublet absorption bands appear in the region of 2850–2950 cm⁻¹ which is due to stretching vibration of aliphatic group and another band at 1350–1480 cm⁻¹ is due to bending vibration of aliphatic group. While the

stretching vibration at 1210–1240 cm⁻¹ is due to the presence of sulphate group from intercalated SDS anion [11]. A strong absorption band at 1364 cm⁻¹ is due to the presence of nitrate as the salt used for the source of metal ions which is zinc nitrate.

Also shown in Figure 2, the FTIR spectra of ZLH-SDS-THI resemble the ZLH-SDS spectra. A strong and broad band at 3473 cm⁻¹ is attributing to the stretching vibration of the hydroxyl group of the water molecule. While a peak at 1625 cm⁻¹ reveals that there is a free water molecule in the interlayer of nanocomposite. A sharp doublet absorption of ZLH-SDS-THI nanocomposite band resembles the peak in ZLH-SDS layer at 2913 and 2846 cm⁻¹ which is due to stretching vibration of the C-H group that presents in the nanocomposite. Whereas the peak at 1460 cm⁻¹ is due to bending vibration of the aliphatic group, C-H. The bands appeared at 1183 and 1056 cm⁻¹ are assigned to the asymmetric and symmetric stretching vibration of S = O [12]. The stretching vibration of S = O for ZLH-SDS-THI particles is shifted to lower frequencies, indicating the configuration variation of the OSO₃⁻ functional group [12]. Those down-shift conforms to the losing of S = O bond strength, referring the existence of a hydrogen bond within ZLH interlayer and sulphate group (S = O H-O-Zn) as well as the electrostatic attraction [12]. The typical absorption peak of thiocloprid peaks that appear at 1001 and 719 cm⁻¹ are due to the stretching vibration of C-N and C-Cl respectively, indicating that thiocloprid molecule have been successfully loaded into the ZLH interlayer. After the intercalation, the peak that represents a cyanide group is disappearing due to nitrile hydrolysis reaction. The electropositive nitrile accepts a nucleophile for addition reaction and undergoes an intermolecular rearrangement to form cyanide ion [25]. The FTIR spectra also confirms the disappearance of nitrate absorption peak at 1364 cm⁻¹ which indicates the successful of ion exchange between nitrate ion and thiocloprid anion.

Spatial orientation

A graphic orientation of DDS anion and thiocloprid anion in the interlayer of zinc hydroxide of the product is shown in Figure 3. The DDS anion adopts a monolayer structure composed of interpenetrating alkyl chains with the oxygen atom of SO₃⁻ groups anchored to positively charged ZLH plane by electrostatic interaction with the hydrocarbon tail expanding outward [12,26]. The negatively charged thiocloprid anion is arranged parallel to DDS anion and electrostatically attracted to ZLH plane. The schemed spatial orientation of thiocloprid in the ZLH interlayer gallery is referring to the basal spacing of the PXRD analysis. Accordingly, the basal spacing of ZLH-SDS-THI is 30.1 Å and the interlayer height of the nanocomposite is estimated to be about 20.1 Å, obtained by subtracting the layer thickness plus the height of a Zn²⁺ moiety of the lattice from the basal spacing [27]; i.e. 21.1 Å = 30.1 – (4.8 + 2.6 + 2.6) Å.

Elemental analysis

Table 2 shows the elemental analysis of ZLH-SDS and ZLH-SDS-THI nanocomposite which contains 2.46% N, 24.80% C, 5.48% H and 3.38% S for ZLH-SDS whereas 19.88% nitrogen, 44.78% carbon, 3.62% hydrogen and 12.41% sulphur for ZLH-

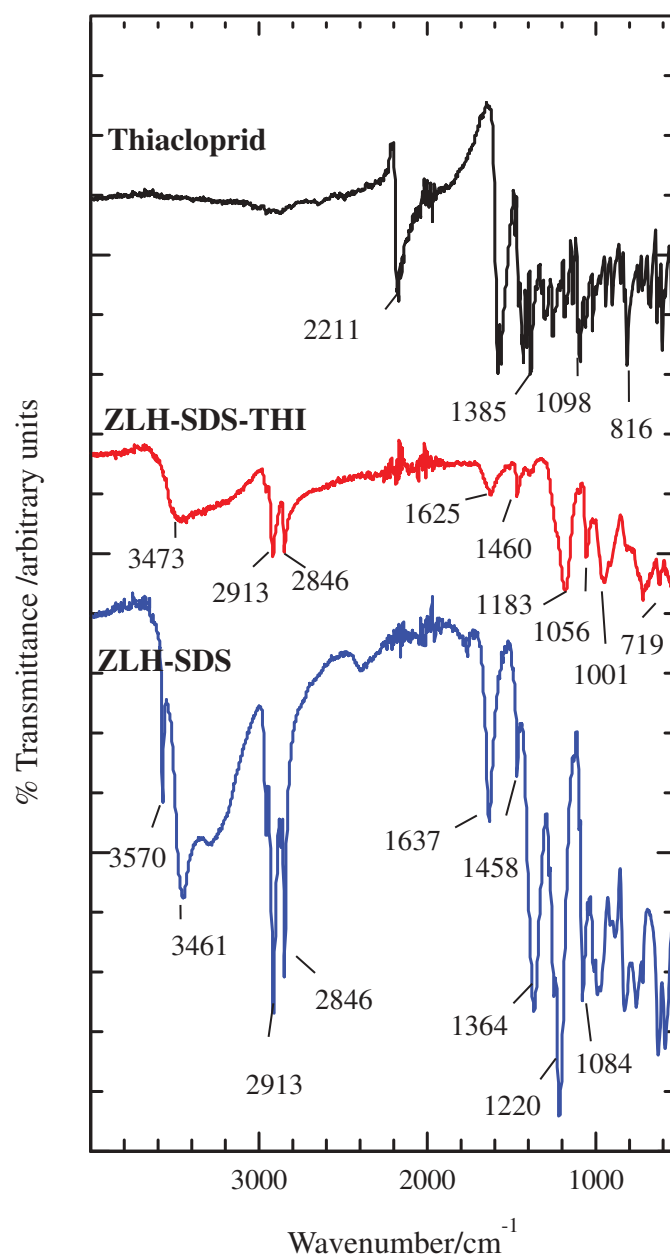


Figure 2. The FTIR spectra for ZLH-SDS, thiocloprid anion and ZLH-SDS-THI nanocomposite.

Table 1. FTIR bands for ZLH-SDS, thiocloprid anion and ZLH-SDS-THI nanocomposite.

Characteristic group	ZLH-SDS (cm ⁻¹)	ZLH-SDS-THI (cm ⁻¹)	Thiocloprid (cm ⁻¹)
ν (O-H), H-bonded	3461	3473	-
ν (O-H) in the interlayer; H ₂ O	3570	-	-
ν (H-O-H) in the interlayer; H ₂ O	1637	1625	-
ν (C \equiv N)	-	-	2211
ν (C-Cl)	-	719	606
ν (C-N)	-	1001	1098
ν (C-H), stretching	2846	2846	-
	2913	2913	-
ν (C-H), bending	1458	1460	1385
ν (N-O)	1364	-	-
ν_{as} (S = O)	1220	1183	-
ν_s (S = O)	1084	1056	-

SDS-THI nanocomposite. Percentage N was used to calculate the loading percentage of thiocloprid in the interlayer of ZLH which was found to be 89.71%.

From ICP-OES analysis, the percentage of Zn in ZLH-SDS-THI nanocomposite was estimated to be 35.63%, respectively. From PXRD and FTIR analysis, the peak for nitrate does no

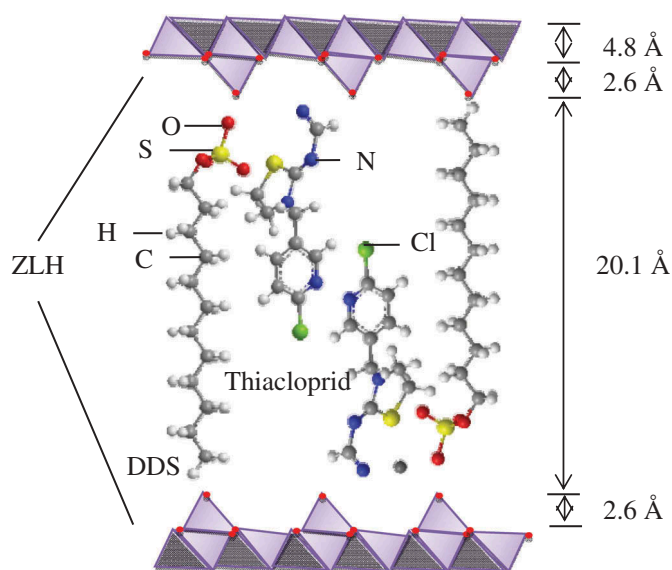


Figure 3. The proposed orientation of thiocloprid and SDS anions intercalated within the ZLH interlayer gallery resulting in ZLH-SDS-THI nanocomposite estimated by Chemoffice software.

Table 2. Compositional data for synthesised ZLH-SDS and ZLH-SDS-THI nanocomposite.

Sample	N (%)	C (%)	H (%)	S (%)	Anion (% w/w)
ZLH-SDS	2.46	24.80	5.48	3.38	-
ZLH-SDS-THI	19.88	44.78	3.62	12.41	89.71

longer exist in the nanocomposite spectra. Therefore, the percentage N in the ZLH-SDS-THI nanocomposite indicates the successful adsolubilisation of thiocloprid into the interlayer of ZLH. The results were also supported by the increasing percentage of C and S. From the elemental analysis and TGA/DTG analysis, the formula of ZLH-SDS-THI nanocomposite was proposed as $\text{Zn}^{2+}(\text{OH})_{1.48}(\text{CH}_3(\text{CH}_2)_{11}\text{SO}_4)^{-}_{0.52}(\text{C}_{10}\text{H}_9\text{ClN}_4\text{S})^{-}_{0.65} \cdot 0.79 \text{H}_2\text{O}$.

Thermal analysis

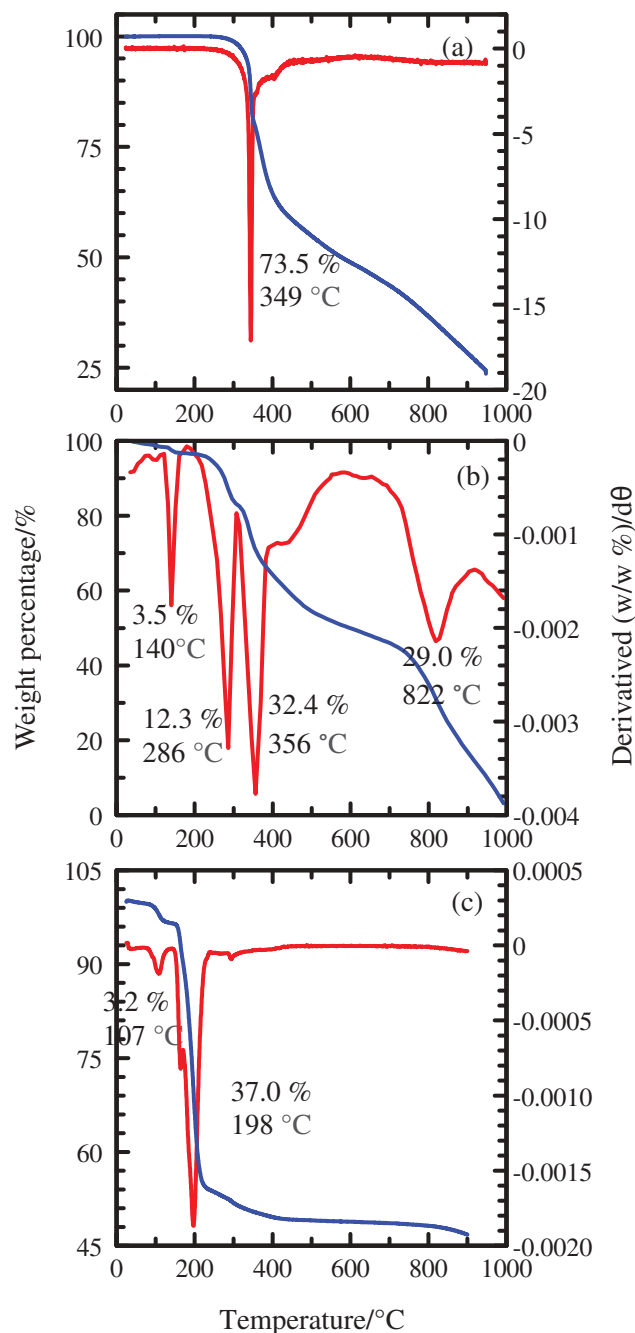
The TGA-DTG curve for thiocloprid, ZLH-SDS-THI nanocomposite and ZLH-SDS are shown in Figure 4. Thermal degradation of pure thiocloprid (Figure 4(a)) was recorded between 263°C and 438°C, showing 73.55% of weight loss at the maximum temperature of 349°C.

Whereas four weight loss in ZLH-SDS-THI nanocomposite were observed, as shown in Figure 4(b). The first weight loss was recorded at 140°C with weight loss of 3.5%, which is attributed to dehydration of physically adsorbed intercalated water [6]. The second weight loss (12.3%) at 286°C corresponds to the decomposition of DDS anion. The maximum temperature of 356°C represents the 32.4% weight loss of thiocloprid anion. The last weight loss (29.0%) is at 822°C (temperature range 680–928°C) which is ascribed to the complete decomposition of amorphous mixture of salts generated during the initial anion decomposition [28,29].

The ZLH-SDS exhibits two weight loss stages (Figure 4(c)). The first (70–119°C) corresponds to the removal of intercalated water at 107°C [6]. The second (154–399°C) is a consequence of the decomposition of DDS anion, companying a weak exothermic peak at 198°C with a 37.0% weight loss. The thermal study of ZLH-SDS-THI nanocomposite revealed that the thiocloprid anion that intercalates in the ZLH-SDS interlayer is thermally stable contrast to its pristine form. This is due to the electrostatic interaction between thiocloprid anions and ZLH layer that act as a heat barrier, thus being responsible for a marked improvement in the thermal stability of the thiocloprid pesticide [13].

Surface morphology analysis

As shown in Figure 5, there is clearly significant difference in the morphology of ZLH-SDS and ZLH-SDS-THI nanocomposite. ZLH-SDS shows a small and plate-like structure with rough surface. Whereas ZLH-SDS-THI nanocomposite shows bright micrograph with some smooth region and different size of plate-like particle. The surface morphology of ZLH-SDS-THI nanocomposite is typically in plate-like structure. It showed that the intercalation of thiocloprid into the interlayer of ZLH-SDS resulted in a changed of surface morphology as previously reported by [1,30].

**Figure 4.** Thermogravimetric curve for thiocloprid anion (a), ZLH-SDS-THI nanocomposite (b) and ZLH-SDS (c).

Surface area analysis

The specific surface area of ZLH-SDS and ZLH-SDS-THI nanocomposite was also studied. The calculated Brunauer-Emmett-Teller (BET) surface areas of this sample are listed in Table 3. The specific BET surface area of ZLH-SDS is 7.027 m²/g. After the intercalation, the value was decreased to 0.872 m²/g. The decrease in surface area of the nanocomposite leads to an increasing pore size and decreasing the pore volume [18].

Based on Figure 6(a), the adsorbate uptake of ZLH-SDS is slow at the relative pressure range of 0.0–0.6, fairly rapid at 0.6–0.9, before rapid adsorption can be observed around >0.9. The optimum uptake is 32 cm³/g, indicating high capacity for the uptake of nitrogen gas. Whereas ZLH-SDS-THI nanocomposite shows a slow uptake around 0.0–0.8, before reaching maximum with rapid uptake at 8.2 cm³/g (Figure 6(b)).

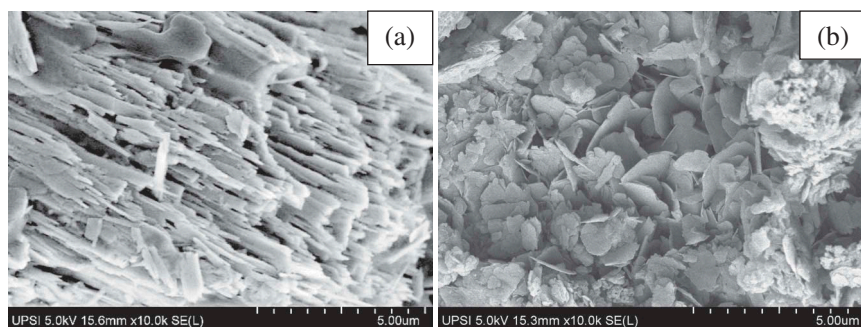


Figure 5. FESEM images of ZLH-SDS (a) and ZLH-SDS-THI (b) 10 k magnification nanocomposite.

Table 3. Surface properties of ZLH-SDS and ZLH-SDS-THI nanocomposite.

Samples	Specific BET surface area (m^2/g)	Average pore diameter (nm)	Classification
ZLH-SDS	7.027	27.83	Mesoporous
ZLH-SDS-THI	0.872	58.16	Macroporous

Different types of the desorption branch of the hysteresis loop for the host and resulting nanocomposite indicate different pore texture between both materials [18,31]. ZLH-SDS exhibit a mesoporous type material with Type IV isotherm. While the resulting nanocomposite exhibit macroporous material with Type II isotherm which attribute to non-porous material with monolayer coverage followed by multilayering at high relative pressure [32].

Figure 7 shows the Barrett-Joyner-Halenda (BJH) desorption pore size distributions for ZLH-SDS and ZLH-SDS-THI nanocomposite. The difference in pore size distribution was observed between ZLH-SDS and ZLH-SDS-THI nanocomposite which is due to the modification of the pore by thiacloprid anion after the adsolubilisation process [31]. This study proves that there is a possibility of adsorption mechanism present on ZLH and the resulting nanocomposite as previously reported by [33].

Controlled release study

The release profiles of thiacloprid anion from interlayer of ZLH-SDS-THI nanocomposite were done into three different concentrations of sodium phosphate (Na_3PO_4), sodium

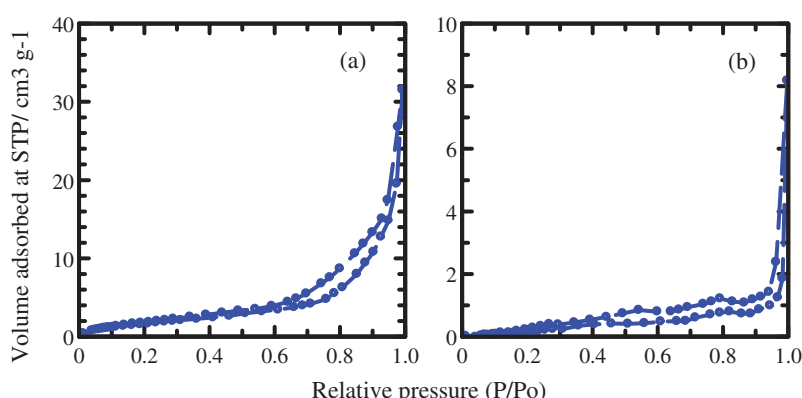


Figure 6. Adsorption-desorption isotherms of nitrogen gas for ZLH-SDS (a) and ZLH-SDS-THI (b).

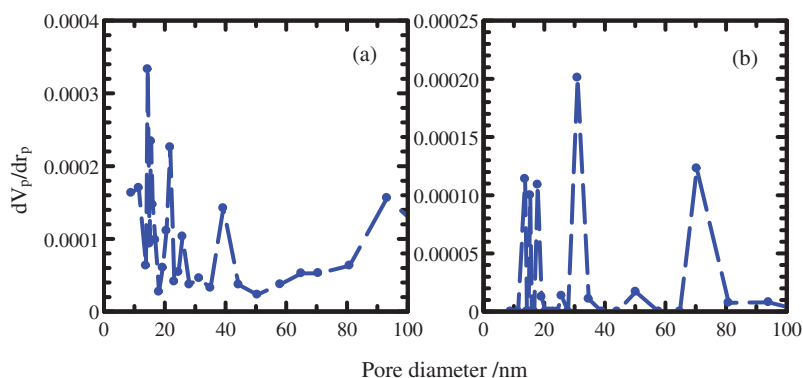


Figure 7. BJH desorption pore size distributions for ZLH-SDS (a) and ZLH-SDS-THI (b).

sulphate (Na_2SO_4) and sodium chloride solution (NaCl). This solution is chosen because sulphate, phosphate and chloride ion are present in the rainwater and the soil composition. These release profiles in phosphate, sulphate and chloride medium are shown in Figure 8.

From Figure 8(a), the release rate of thiocloprid from interlayer of ZLH in 0.1, 0.2 and 0.3 M phosphate solution was faster at the first 500 min before reaching equilibrium at around 1500 min. In Figure 8(b), the release of thiocloprid in sulphate solution was found to be faster at the beginning, until reaching the equilibrium at around 1200 min for all three concentrations. As for as chloride solution in Figure 8(c), the release of thiocloprid is faster at first 500 min before reaching equilibrium point. The fast release for all solutions is possibly due to the high density of incoming anion leading to rapid ion exchange process of thiocloprid in the interlayer of ZLH with incoming anions in the phosphate, sulphate and chloride solution. The extended time period for thiocloprid to release from ZLH matrix is possibly due to the strong host-guest interaction which is the electrostatic attraction between the positive charge ZLH and negative charge of anionic thiocloprid leading to much slower release process [34,35].

As shown in Figure 8, it is observed that release of thiocloprid into phosphate solution dominates the accumulate release percentage with 68.3%, 75.6% and 90.0% in 0.1, 0.2 and 0.3 M concentration, respectively, compared to sulphate and chloride solution. The percentage accumulated release of thiocloprid into sulphate solution are 36.7%, 57.9% and 87.6% in 0.1, 0.2 and 0.3 M, respectively, meanwhile in chloride solution the percentage of accumulate release are 10.9%, 30.8% and 37.4% in 0.1, 0.2 and 0.3 M, respectively. The percentage of accumulated thiocloprid was found to be reliant on the anion in the aqueous solutions in the order of $\text{PO}_4^{3-} > \text{SO}_4^{2-} > \text{Cl}^-$. The result showed that the affinity of anion in the solution plays an important rule for controlled release of thiocloprid anion from interlayer of ZLH. The exchange ability of incoming anions increases with increasing charge density and decreasing ionic radius which indicates phosphate has higher affinity followed by sulphate and lastly chloride ion [36–38]. In other word, the affinity of incoming anion induces the ion exchange process and subsequently determines the amount of the guest anion to be released [36]. The high charge density of phosphate, sulphate, and chloride anion leading to a high formation of

electrostatic interaction between incoming anion (phosphate, sulphate, and chloride) and the positively charged layer of ZLH in the ion exchange process [37,38].

Kinetic study

Kinetic study of thiocloprid releases from the interlayer of ZLH-SDS-THI nanocomposite is further performed in order to understand the release behaviour of thiocloprid into different aqueous solutions. The quantitative analysis of the data obtained from the release study is fitted to zeroth order (Equation (5)) [39], first order (Equation (6)) [40], pseudo second order (Equation (7)) [41], parabolic diffusion model (Equation (8)) [42] and Fickian diffusion model (Equation (9)) [43] for which the equations are given in the following:

$$x = t + C \quad (5)$$

$$-\log (1 - M_i/M_f) = t + C \quad (6)$$

$$t/M_i = 1/M_f^2 + t/M_f \quad (7)$$

$$M_i/M_f = kt^{0.5} + C \quad (8)$$

$$M_i/M_f = kt^n \quad (9)$$

x is the percentage release of the thiocloprid anion at time t , M_i and M_f are the initial and final concentration of thiocloprid anions, respectively, and C is a constant. Whereas M_i/M_f represents the fraction of release anion at time, t , and n is an empirical parameter describing the release mechanism (Silion et al. 2012). The resulting correlation coefficient, r^2 values and the parameters obtained from the fitting are shown in Table 4. The rate constant k , and $t_{1/2}$ are calculated from the corresponding equation where $t_{1/2}$ is the time required for 50% of thiocloprid to be released from ZLH-SDS-THI nanocomposite. The diffusional exponent, n and k for Fickian diffusion model have been evaluated from the slope of the plot $\ln(M_i/M_f)$ versus $\ln t$.

The obtained fitting curve between 0 and 500 min is presented in Figure 9. The best fit graph can be obtained through the value of r^2 , where the closest value to 1 is

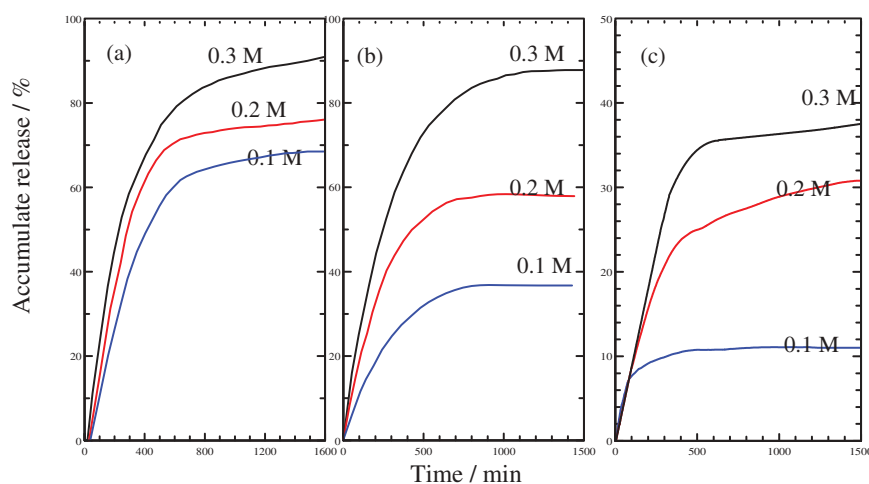
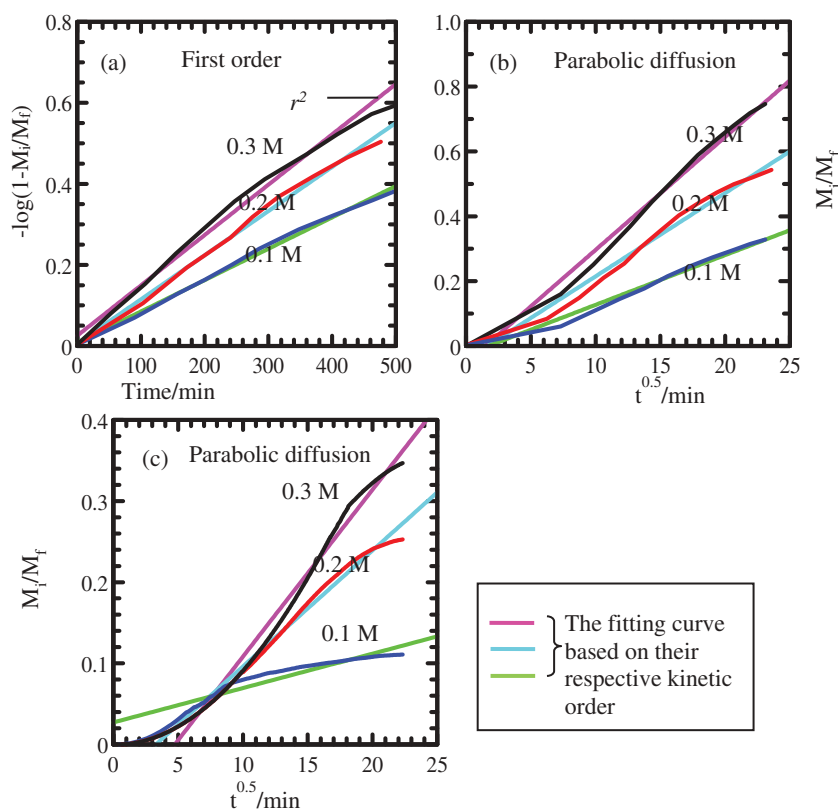


Figure 8. Release profile of thiocloprid from ZLH-SDS-THI nanocomposite into 0.1, 0.2 and 0.3 M concentration of aqueous (a) Na_3PO_4 , (b) Na_2SO_4 and (c) NaCl solutions.

Table 4. The rate constants (k), half-life ($t_{1/2}$) and correlation coefficients (r^2) obtained from the fitting data of thiacloprid release from ZLH-SDS-THI nanocomposite into Na_3PO_4 , Na_2SO_4 and NaCl solutions.

Na_3PO_4 (M)	Zeroth order	Pseudo second order	Parabolic diffusion	Fickian	First order			
					r^2	$k (\times 10^{-4})$ ($\text{mol}^{-1}\text{L s}^{-1}$)	$t_{1/2}(\text{min})$	c ($\times 10^{-3}$)
0.1	0.971	0.296	0.965	0.969	0.996	7.74	231.4	7.59
0.2	0.952	0.550	0.972	0.969	0.995	10.9	224.3	6.09
0.3	0.939	0.627	0.985	0.967	0.991	12.4	205.1	5.30
Na_2SO_4 (M)	Zeroth order	First order	Pseudo second order	Fickian	Parabolic diffusion			
					r^2	$k (\times 10^{-2})$ ($\text{mol}^{-1}\text{L s}^{-1}$)	$t_{1/2}(\text{min})$	$c (\times 10^{-2})$
0.1	0.958	0.976	0.758	0.985	0.982	1.53	13.0	2.67
0.2	0.942	0.977	0.788	0.976	0.981	2.57	12.6	4.23
0.3	0.956	0.998	0.812	0.962	0.988	3.48	12.3	5.20
NaCl (M)	Zeroth order	First order	Pseudo second order	Fickian	Parabolic diffusion			
					r^2	$k (\times 10^{-2})$ ($\text{mol}^{-1}\text{L s}^{-1}$)	$t_{1/2}(\text{min})$	$c (\times 10^{-2})$
0.1	0.706	0.719	0.005	0.847	0.861	0.42	13.8	2.72
0.2	0.94	0.953	0.001	0.982	0.988	1.43	12.3	4.70
0.3	0.972	0.982	0.011	0.995	0.981	2.06	7.2	9.75

**Figure 9.** The best fitted of the thiacloprid release data into 0.1, 0.2 and 0.3 M concentration of aqueous (a) Na_3PO_4 (first order), (b) Na_2SO_4 (parabolic diffusion) and (c) NaCl solutions (parabolic diffusion).

considered as best fit as listed in Table 4. The correlation coefficient, r^2 for the release of thiacloprid into phosphate solution shows the release profile followed the first order (Figure 9(a)). Whereas the release of thiacloprid from inter-layer of ZLH-SDS-THI nanocomposite into sulphate (Figure 9(b)) and chloride (Figure 9(c)) solution followed the parabolic diffusion model.

The first-order model demonstrates the release system where dissolution rate depends only on one reactant concentration [28]. As shown in Table 4, it is obvious that the rate constant depends on the concentration phosphate solution. The rate constant increases as the concentration of anion increases. While the $t_{1/2}$ is decreases as more phosphate ions

are available to be ion exchanged with thiacloprid anion resulting in lower $t_{1/2}$ values[37].

On the other hand, the parabolic diffusion model clarifies that the release process is controlled by intraparticle diffusion or surface diffusion which indicate that the external surface diffusion or the intraparticle diffusion via ion exchange is the rate-determining step in the release process [35,37]. The electrostatic interaction between host and guest is a factor affecting the diffusion rate of the intercalated species [44]. This interaction can be shown by the presence of coordinative unsaturated $\text{Zn}(\text{OH})_3$ units of ZLH lattice, leads to the formation of a coordination bond between the exposed Zn^{2+} ions and

cyanide groups of thiacloprid. Such a strong interaction has significant contribution to the decrease of release coefficient in the ZLH-based materials. Similar to the release of thiacloprid into the phosphate solution, the rate constant of thiacloprid release into the sulphate and chloride solutions increased while the $t_{1/2}$ decreased as the concentration of solution increased.

Conclusion

The adsolubilisation of thiacloprid into the gallery of ZLH is successful with the aid of surfactant, SDS with a basal spacing of 30.1 Å to accommodate thiacloprid in a monolayer arrangement. The FTIR study showed the presence of functional groups for both guest anions and inorganic host which also supported the intercalation of thiacloprid within the interlayer gallery of ZLH. The percentage loading is estimated to be 89.71% and the intercalation of thiacloprid was supported by the presence of nitrogen. An enhanced thermal stability of thiacloprid in the ZLH interlayer was highlighted in the thermogravimetric analysis. The release of thiacloprid from its nanocomposite is controlled by first-order kinetics for phosphate medium and parabolic diffusion model for sulphate and chloride medium. Therefore, this study proves that ZLH can be a good host for thiacloprid anions and can be used in controlled release of thiacloprid pesticides.

Acknowledgments

The author is grateful to the support for the research provided by UPSI under FRGS Grant No. 2019-0002-102-02. ZM thanks UPSI for all funding and support for this research.

Disclosure statement

No potential conflict of interest was reported by the authors.

Funding

This work was supported by the Universiti Pendidikan Sultan Idris [2019-0002-102-02].

Notes on contributors

Zuhailimuna Muda received her bachelor degree from Sultan Idris Education University (Tanjong Malim, Malaysia) in 2013, and received her Master degree at the same university in 2015. He is a PhD candidate supervised by Associate Professor Dr. Norhayati Hashim at the same university. His current research interest is synthesis of zinc layered hydroxide-based nanomaterials used for controlled release formulation of pesticides.

Norhayati Hashim received a PhD degree at University Putra Malaysia in 2012 and joined the Nanotechnology Research Centre the same year. She is now a senior lecturer at Sultan Idris Education University and currently serves as head of chemistry department. She has expertise in the nanomaterial and inorganic chemistry. Her current research concentrates on synthesis, characterization, and controlled release formulation of various active agents.

Ilyas Md Isa received a PhD degree at Universiti Sains Malaysia in 2010. He is now a Professor at Sultan Idris Education University and currently serves as Deputy Academic and International Dean of the Faculty of Science and Mathematics. He is expertise in analytical chemistry, chemical and biosensor.

Suzaliza Mustafar received a PhD degree at University of Tokyo. She is senior lecturer at Sultan Idris Education University in chemistry department and expertise in photochemistry, coordination complexes, electrochemistry, and material chemistry.

Suriani Abu Bakar received a PhD degree at Universiti Teknologi MARA in 2011. She is senior lecturer at Sultan Idris Education University in physics department. Currently, her research interest concentrates on carbon nanotubes, graphene, vertically aligned carbon nanotubes from palm oil/waste cooking palm oil using Thermal Chemical Vapor Deposition (TCVD) method, hydrogenated amorphous carbon thin Films (a-C:H), Diamond-like Carbon Films (DLC), and Plasma Enhanced Chemical Vapor Deposition Technique (PECVD).

Mazidah Mamat is a senior lecturer at Universiti Malaysia Terengganu in School of Fundamental Science. She is expertise in material characterization. Her current research focus on layered double hydroxide for adsorption of hazardous materials.

Mohd Zobir Hussein obtained his PhD degree from University of Reading, U.K. and spent his postdoctoral/research attachments on nanomaterials and their applications at various laboratories, namely University of Southampton, U.K., Pennsylvania State University, USA, Victoria University of Wellington, New Zealand and University of Western Australia, Australia. He is currently the program manager for nanomaterials at the Materials Synthesis and Characterization Laboratory, Institute of Advanced Technology (ITMA), UPM. He and his research group focusing their research works on nanomedicine, especially for theranostics delivery systems, nanomaterials for thermal energy storage and agronanochemicals. His research interests are in the design, synthesis and applications to improve drug and diagnostic agents' bioavailability and efficacy by nanotechnology platforms.

References

- [1] Hashim N, Muda ZI, et al. The effect of ion exchange and co-precipitation methods on the intercalation of 3-(4-methoxyphenyl)propionic acid into layered zinc hydroxide nitrate. *J Porous Mater.* **2018**;25:249–258.
- [2] Cao Y, Li G, Li X. Graphene/layered double hydroxide nanocomposite: properties, synthesis, and applications. *Chem Eng J.* **2016**;292:207–223.
- [3] Senapati S, Thakur R, Verma SP, et al. Layered double hydroxides as effective carrier for anticancer drugs and tailoring of release rate through interlayer anions. *J Control Release.* **2016**;224:186–198.
- [4] Cunha VRR, Guilherme VA, De Paula E, et al. Delivery system for mefenamic acid based on the nanocarrier layered double hydroxide: physicochemical characterization and evaluation of anti-inflammatory and antinociceptive potential. *Mater Sci Eng C.* **2016**;58:629–638.
- [5] Nabipour H, Sadr MH, Thomas N, et al. Synthesis, characterisation and sustained release properties of layered zinc hydroxide intercalated with amoxicillin trihydrate. *J Exp Nanosci.* **2015**;10(16):1269–1284.
- [6] Nabipour H, Sadr MH. Controlled release of diclofenac, an anti-inflammatory drug by nanocompositing with layered zinc hydroxide. *J Porous Mater.* **2015**;22(2):447–454.
- [7] Liu J, Zhang X, Zhang Y. Preparation and release behavior of chlorpyrifos adsorbed into layered zinc hydroxide nitrate intercalated with dodecylbenzenesulfonate. *ACS Appl Mater Interfaces.* **2015**;7(21):11180–11188.
- [8] Arizaga GGC, Gardolinski JEFDC, Schreiner WH, et al. Intercalation of an oxalatoxonobate complex into layered double hydroxide and layered zinc hydroxide nitrate. *J Colloid Interface Sci.* **2009** Feb;330(2):352–358.
- [9] Babakhani S, Talib ZA, Hussein MZ, et al. Synthesis and characterization of Zn-Al layered double hydroxide (LDH) nanocomposite intercalated with sodium dodecyl sulfate (SDS). *Adv Mater Res.* **2014**;1024:52–55.
- [10] Terrin MM, Poli AL, Jr MA H, et al. Effect of the loading of organomodified clays on the thermal and mechanical properties of a model dental resin. *Mater Res.* **2016**;19(1):40–44.

- [11] Hussein MZ, Zainal Z, Ming CY. Microwave-assisted synthesis of Zn-Al-layered double hydroxide-sodium dodecyl sulfate nanocomposite. *J Mater Sci Lett*. **2000**;19(10):879–883.
- [12] Zhao J, Fu X, Zhang S, et al. Water dispersible avermectin-layered double hydroxide nanocomposites modified with sodium dodecyl sulfate. *Appl Clay Sci*. **2011**;51(4):460–466.
- [13] Monteiro MKS, Oliveira VRLD, Santos FKGD, et al. Analysis of water barrier, mechanical and thermal properties of nanocomposites based on cassava starch and natural clay or modified by anionic exchange. *Mater Res*. **2017**.
- [14] Abramović BF, Banić ND, Šojić DV. Degradation of thiacloprid in aqueous solution by UV and UV/H₂O₂ treatments. *Chemosphere*. **2010**;81(1):114–119.
- [15] Li B, Wang W, Wang K, et al. Thiacloprid suspension formula optimization by a response surface methodology. *RSC Adv*. **2015**;5(34):26654–26661.
- [16] Faria DM, Dourado Júnior SM, Nascimento JPLD, et al. Development and evaluation of a controlled release system of thb herbicide using alginate microparticles. *Mater Res*. **2017**;20(1):225–235.
- [17] Englert D, Bundschuh M, Schulz R. Thiacloprid affects trophic interaction between gammarids and mayflies. *Environ Pollut*. **2012**;167:41–46.
- [18] SHH AA, Al-Qubaisi M, Hussein MZ, et al. Preparation of hippurate-zinc layered hydroxide nanohybrid and its synergistic effect with tamoxifen on HepG2 cell lines. *Int J Nanomedicine*. **2011**;6(1):3099–3111.
- [19] Cursino ACT, Rives V, Arizaga GGC, et al. Rare earth and zinc layered hydroxide salts intercalated with the 2-aminobenzoate anion as organic luminescent sensitizer. *Mater Res Bull*. **2015**;70:336–342.
- [20] Moezzi A, Cortie M, McDonagh AM. Formation of zinc hydroxide nitrate by H⁺-catalyzed dissolution-precipitation. *Eur J Inorg Chem*. **2013**;2013(8):1326–1335.
- [21] Liang C, Tian Z, Tsuruoka T, et al. Blue and green luminescence from layered zinc hydroxide/dodecyl sulfate hybrid nanosheets. *J Photochem Photobiol A Chem*. **2011**;224(1):110–115.
- [22] Krishnamoorti R, Banik I, Xu L, et al. Rheology and processing of polymer nanocomposites. *Rev Chem Eng*. **2010**;26:3–12.
- [23] Arizaga GGC, Satyanarayana KG, Wypych F. Layered hydroxide salts: synthesis, properties and potential applications. *Solid State Ion*. **2007**;178(15–18):1143–1162.
- [24] Yang W, Ma L, Song L, et al. Fabrication of thermoplastic polyester elastomer/layered zinc hydroxide nitrate nanocomposites with enhanced thermal, mechanical and combustion properties. *Mater Chem Phys*. **2013**;141(1):582–588.
- [25] Prihod'ko R, Sychev M, Kolomitsyn I, et al. Layered double hydroxides as catalysts for aromatic nitrile hydrolysis. *Microporous Mesoporous Mater*. **2002**;56(3):241–255.
- [26] Demel J, Hyněk J, Kovář P, et al. Insight into the structure of layered zinc hydroxide salts intercalated with dodecyl sulfate anions. *J Phys Chem C*. **2014**;118(46):27131–27141.
- [27] Mohsin SMN, Hussein MZ, Sarijo SH, et al. Synthesis of (cinnamate-zinc layered hydroxide) intercalation compound for sunscreen application. *Chem Cent J*. **2013**;7:26–38.
- [28] Latip AFA, Hussein MZ, Stanslas J, et al. Release behavior and toxicity profiles towards A549 cell lines of ciprofloxacin from its layered zinc hydroxide intercalation compound. *Chem Cent J*. **2013**;7(1):119–130.
- [29] Demel J, Kubát P, Jirka I, et al. Inorganic-organic hybrid materials: layered zinc hydroxide salts with intercalated porphyrin sensitizers. *J Phys Chem C*. **2010**;114(39):16321–16328.
- [30] Ghotbi MY, Bagheri N, Sadrnezhad SK. Zinc-stearate-layered hydroxide nanohybrid material as a precursor to produce carbon nanoparticles. *J Alloys Compd*. **2011**;509(5):2441–2444.
- [31] Mamat M, Kusriani E, Yahaya A, et al. Intercalation of anthranilate ion into zinc-aluminium-layered double hydroxide. *Int J Technol*. **2013**;1:73–80.
- [32] Koilraj P, Sasaki K, Srinivasan K. Novel biomolecule-assisted interlayer anion-controlled layered double hydroxide as an efficient sorbent for arsenate removal. *J Mater Chem A*. **2017**;5(28):14783–14793.
- [33] Herald E, Suprihatin RWW, Pranoto. Intercalation of diclofenac in modified Zn/Al hydrotalcite-like preparation. *IOP Conf Ser Mater Sci Eng*. **2016**;107(1):1–7.
- [34] Hashim N, Misuan NS, Md Isa I, et al. Development of a novel nanocomposite consisting of 3-(4-methoxyphenyl)propionic acid and magnesium layered hydroxide for controlled-release formulation. *J Exp Nanosci*. **2016**;11(10):776–797.
- [35] Kong X, Shi S, Han J, et al. Preparation of glycyl-L-tyrosine intercalated layered double hydroxide film and its in vitro release behavior. *Chem Eng J*. **2010**;157(2–3):598–604.
- [36] Sarijo SH, Hussein MZ, Yahaya AHJ, et al. Effect of incoming and outgoing exchangeable anions on the release kinetics of phenoxyherbicides nanohybrids. *J Hazard Mater*. **2010**;182(1–3):563–569.
- [37] Hashim N, Hussein MZ, Isa I, et al. Synthesis and controlled release of cloprop herbicides from cloprop-layered double hydroxide and cloprop-zinc-layered hydroxide nanocomposites. *Open J Inorg Chem*. **2014**;2014(January):1–9.
- [38] Sarijo SH, Ghazali SAISM, Hussein MZ, et al. Synthesis of nanocomposite 2-methyl-4-chlorophenoxyacetic acid with layered double hydroxide: physicochemical characterization and controlled release properties. *J Nanopart Res*. **2013**;15(1):1536.
- [39] Atkins PW, Paula JD. *Physical chemistry*. 7th ed. Oxford: Oxford University press; **2002**.
- [40] Costa P, Sousa Lobo JM. Modeling and comparison of dissolution profiles. *Eur J Pharm Sci*. **2001**;13(2):123–133.
- [41] Ho YS. Review of second-order models for adsorption systems. *J Hazard Mater*. **2006**;136(3):681–689.
- [42] Kodama T, Harada Y, Ueda M, et al. Selective exchange and fixation of strontium ions with ultrafine Na-4-mica. *Langmuir*. **2001**;17(16):4881–4886.
- [43] Ritger PL, Peppas NA. A simple equation for description of solute release II. Fickian and anomalous release from swellable devices. *J Control Release*. **1987**;5(1):37–42.
- [44] Yang JH, Han YS, Park M, et al. New inorganic-based drug delivery system of indole-3-acetic acid-layered metal hydroxide nanohybrids with controlled release rate. *Chem Mater*. **2007**;19(10):2679–2685.